

Study of the critical-fields and the thermal broadening in polycrystalline $\text{Ag}_2\text{FeGeSe}_4$ semiconducting compound

J. Marquina^a, N. Sierralta^b, M. Quintero^c, C. Rincón^c, M. Morocoima^c, and E. Quintero^c

^a*Centro de Estudios Avanzados en Óptica, Departamento de Física, Facultad de Ciencias, Universidad de Los Andes, Mérida 5101, Venezuela.*

^b*Grupo de Teoría de la Materia Condensada, Departamento de Física, Facultad de Ciencias, Universidad de Los Andes, Mérida 5101, Venezuela.*

^c*Centro de Estudios de Semiconductores, Departamento de Física, Facultad de Ciencias, Universidad de Los Andes, Mérida 5101, Venezuela.*

Received 2 February 2017; accepted 30 June 2017

We show that a phenomenological model based on sublattice magnetization describes the temperature and field dependent magnetism in the $\text{Ag}_2\text{FeGeSe}_4$ semiconductor compound with wurtz-stannite-type structure. The model successfully finds the antiferromagnetic (AF), spin flop (SF) and paramagnetic (P) phases for all magnetization curves below the Néel temperature. The Langevin classical function instead of the Brillouin one is used in the analysis of the phase transitions to take into account the randomness of the magnetic moments given the polycrystalline nature of the samples. The critical-fields and the thermal broadening of the phase transitions were also found. The model was tested in the $\text{Ba}_3\text{Cu}_3\text{In}_4\text{O}_{12}$ and $\text{Ba}_3\text{Cu}_3\text{Sc}_4\text{O}_{12}$ compounds, and was successfully identified AF, SF and P phases in these materials.

Keywords: Magnetic semiconductors; antiferromagnetic; magnetization curves.

Hemos demostrado que un modelo fenomenológico basado en la magnetización de la subred describe el magnetismo dependiente del campo y la temperatura en el compuesto semiconductor $\text{Ag}_2\text{FeGeSe}_4$ con estructura tipo wurtz-estanita. El modelo exitosamente encuentra las fases anti ferromagnéticas (AF), espín-flop (SF) y paramagnética (P) para todas las curvas de magnetización por debajo de la temperatura de Néel. Se utiliza la función clásica de Langevin en lugar de la función de Brillouin en el análisis de las transiciones de fases a fin de tomar en cuenta la aleatoriedad de los momentos magnéticos dada la naturaleza policristalina de las muestras. También se encontraron los campos críticos y los anchos térmicos de las transiciones de fases. El modelo fue probado en los compuestos $\text{Ba}_3\text{Cu}_3\text{In}_4\text{O}_{12}$ y $\text{Ba}_3\text{Cu}_3\text{Sc}_4\text{O}_{12}$ y se identificaron exitosamente las fases AF, SF y P en estos materiales.

Descriptores: Semiconductores magnéticos; antiferromagnético; curvas de magnetización.

PACS: 75.50.Pp; 75.50.Ee; 75.60.Ej

1. Introduction

The orthorhombic semiconductor $\text{Ag}_2\text{FeGeSe}_4$ which crystallizes with the wurtz-stannite structure [1,2] belongs to family of the $\text{I}_2\text{-II-IV-VI}_4$ compounds where I = Cu or Ag; II = Zn, Cd, Hg, Mn, Fe or Co; IV = Si, Ge, Sn or Pb; and VI = S, Se or Te. These materials are of great interest because of both their applications in the fabrication of low cost solar cells [3] and their large magneto-optical effects which are observed when II atoms are paramagnetic ions [4,5]. The study of the magnetization of $\text{Ag}_2\text{FeGeSe}_4$ over the temperature range from 2 to 300 K shows that this material has an antiferromagnetic behavior [6]. The large numbers of known antiferromagnetic substances exhibit a rich variety of magnetic phase transitions. These transitions are described with particular emphasis in uniaxial antiferromagnets of the easy-axis type. Susceptibility measurements made at high magnetic field (5 T) showed a magnetic moment of $4.4 \mu_B$ for ion Fe^{+2} in acceptable agreement with the theoretical value of $4.9 \mu_B$ obtained when $J = S$. Measurements of magnetization at high field pulsed technique up to 32 T have also been made on this compound [6].

The present paper describes the behavior of the critical-fields and the thermal broadening for $\text{Ag}_2\text{FeGeSe}_4$ at various

temperatures obtained in a previous work [6]. To our knowledge, there are no previous reports on thermal broadening in $\text{Ag}_2\text{FeGeSe}_4$ compound, and the literature information on it is very scarce.

2. Theoretical details

Theoretical and experimental analysis *e.g.* [4,7-9] for an antiferromagnetic material show that three phases can occur in the magnetic field-temperature ($B - T$) plane of the magnetic phase diagram. These are the paramagnetic (P), the antiferromagnetic (AF) and the spin-flop (SF). At the AF to SF first-order phase transition the magnetization increases linearly with applied field and show a discontinuity, whereas the SF to P phase transition is of second-order type and the magnetization breaks off from this line [10]. These analyzes have been concerned mainly with uniaxial materials with an easy-axis z . It is seen in such a case that the details of the diagram depend on the orientation of the applied magnetic field with the z direction. Critical fields for these transitions are obtained as a function of temperature and the phase diagram in the $B - T$ plane can thus be determined.

According to the scheme proposed by Ehrenberg *et al.* [7], for sufficiently low-fields in the AF region, the magne-

tization is proportional to the applied magnetic field as given by the expression,

$$M_{AF}(B) = (\chi/\mu_0)B, \quad (1)$$

where μ_0 is the permeability of free space and χ is the magnetic susceptibility of the AF ground state often tabulated in terms of the mass susceptibility $\chi_g = \chi/\rho$. Here ρ is the mass density which is $6.83 \times 10^3 \text{ kg/m}^3$ for $\text{Ag}_2\text{FeGeSe}_4$ as calculated from the lattice parameters reported in Ref. 2.

On the other hand, for sufficiently high fields, the magnetic moments are forced into a ferromagnetic-like arrangement, which belongs to the P region in the phase diagram, where all the magnetic moments are aligned with the magnetic field. In this paramagnetic region, the expressions usually applied to single crystals for describing the field and temperature dependence of the magnetization, based on a quantum mechanical description of the phenomena through the function of Brillouin are expected to be inappropriate for polycrystalline samples. This is because polycrystals are macroscopic objects that combine thousands of spins at random. The simplest approximation in such a case is an isotropic distribution of easy axes at angle θ from the applied field B . Therefore, a classical explanation via the Langevin function is justified. Thus, the field and temperature dependence of magnetization in this phase can be expressed as

$$M_p(B, T) = M_s L(x), \quad (2)$$

where M_s is the saturation magnetization and $L(x)$ is the Langevin function which is given by

$$L(x) = \coth(x) - 1/x, \quad (3)$$

with $x = \mu B k_B / T$, μ is the magnetic moment, k_B is the Boltzmann constant and T is the absolute temperature.

Finally, in the SF phase, the magnetization is proportional to the applied field strength corrected in real systems by an offset M_0 :

$$M_{SF}(B) = \alpha B + M_0. \quad (4)$$

For all magnetizations curves below of the Néel temperature the field dependence of the magnetization, assuming the existence of an SF phase, can be described by the following expression:

$$\begin{aligned} M(B) = & (1/4)\{M_{AF}(B)[1 - \tanh((B - B_{SF})/\sigma_{SF})] \\ & \times [1 - \tanh((B - B_P)/\sigma_P)] \\ & + M_{SF}(B)[1 + \tanh((B - B_{SF})/\sigma_{SF})] \\ & \times [1 - \tanh((B - B_P)/\sigma_P)] \\ & + M_P(B)[1 + \tanh((B - B_{SF})/\sigma_{SF})] \\ & \times [1 + \tanh((B - B_P)/\sigma_P)]\} \end{aligned} \quad (5)$$

Here B_{SF} and B_P are the critical field strengths for the transitions AF→SF and SF→P, σ_{SF} and σ_P are a measure for the width of the thermal broadening of these transitions.

3. Results and Discussion

The magnetization of $\text{Ag}_2\text{FeGeSe}_4$ at 2 K as a function of the applied magnetic field is shown in Fig. 1a). Only the up-stroke cycle is presented in this figure. The application of the external field induces the two successive AF→SF and SF→P phase transitions expected for this compound. These are observed at about 16 and 25 T, respectively. The stability

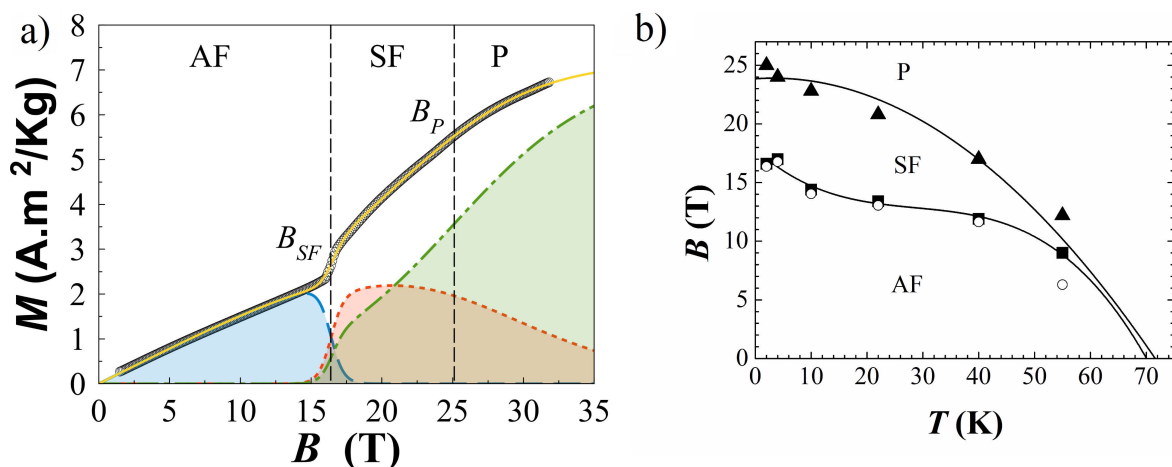


FIGURE 1. (a) Magnetization M against external applied magnetic field B at 2 K from pulsed field measurements for upstroke cycle. The dashed vertical lines show the positions of the B_{SF} and B_P points (see Table I). The solid yellow line is a fit of the data (open circles) by using Eq. (5) extrapolated until 35 T. The contributions from the three terms: M_{AF} (dash blue line), M_{SF} (dot red line) and M_P (dash-dot green line) are also shown. (b) The magnetic phase diagram for the $\text{Ag}_2\text{FeGeSe}_4$ compound showing the experimental values for field-up (full points) and the calculated values (open circles) for up-stroke cycle from Table I. The solid lines are guides for eyes extrapolated until the Néel point. Adapted from Ref. 6.

TABLE I. Parameters obtained from fitting Eq. (5) to curves M vs. B at various temperatures. The B_P parameter was taken from the Ref. 6 and the μ parameter was fixed at $\mu_{\text{exp.}} = 4.90$ (Fe^{+2}). Numbers in parentheses are statistical errors. For B_P values was estimated an error of ± 2 T.

T (K)		χ (m^3/Kg) ($\times 10^{-3}$)	α (m^3/Kg) ($\times 10^{-3}$)	M_0 ($\text{A.m}^2/\text{Kg}$) ($\times 10^{-3}$)	M_s ($\text{A.m}^2/\text{Kg}$)	B_{SF} (T)	B_P (T)	σ_{SF} (T)	σ_P (T)	K (Joul/kg)
2	U	1.373(6)	1.21(4)	4(10)	7.26(2)	16.39(3)	24	1.03(3)	9.7(2)	-0.022
	D	2.24(4)	1.48(6)	4(2)		10.95(3)		1.35(3)	20(1)	-0.046
4	U	1.237(3)	1.16(3)	4.9(7)	7.19(2)	16.76(2)	24	1.39(2)	9.0(2)	-0.011
	D	2.02(3)	1.78(5)	-5(1)		10.57(4)		1.50(5)	21(1)	-0.013
10	U	0.968(8)	1.20(6)	-1(1)	6.55(2)	14.03(5)	22	1.82(4)	11.5(5)	0.023
	D	1.30(2)	1.38(7)	1(2)		12.40(6)		2.10(5)	15(1)	0.006
22	U	1.17(2)	1.57(6)	-5(1)	7.49(2)	13.05(3)	21	1.81(3)	15.0(7)	0.034
	D	1.20(2)	1.39(7)	2(1)		12.79(6)		2.14(5)	13(1)	0.016
40	U	1.240(5)	1.54(4)	3.6(7)	9.682(2)	11.63(5)	17	1.93(3)	5.5(2)	0.020
	D	1.409(6)	2.11(2)	-3.8(3)		10.89(3)		1.88(5)	8.0(2)	0.042
55	U	1.1(4)	2.2(7)	5(3)	10(6)	6.3(6)	12	6.8(4)	32(59)	0.022
	D	0.9(2)	2.14(3)	5.2(6)		5.8(4)		7.9(3)	26.0(6)	0.021

Note. The labels U and D mean up-stroke and down-stroke cycles, respectively.

ranges of these phases are summarized in the phase diagram of Fig. 1b).

The solid yellow line in Fig. 1a) represents a fit of Eq. (5) to the experimental $M(B)$ data. It is clear from this figure that the saturation magnetization was not reached in the range of magnetic field values achieved in this work. Also, an appreciable hysteresis effect was observed for all curves (see Fig. 2 in Ref. 6). For this reason, the M_s values were fixed during the fitting for all the curves in the down-stroke cycle, not shown here, at the values obtained in the up-stroke cycle.

Table I summarizes the results obtained by fitting with Eq. (5) the curves of magnetization at various temperatures for up-stroke cycles. The susceptibilities calculated and the critical field strength B_{SF} agree with the experimental values previous report in Ref. 6. It is worth mentioning that attempt

was also made to adjust the magnetizations curves by using the Brillouin function. However, no fit was obtained. This is probably due to the polycrystalline nature of the present sample as was explained above.

For a uniaxial antiferromagnet of the easy-axis type, at temperatures below the Neel temperature T_N , the orientation of M_1 and M_2 relative to the crystallographic axes is determined by the anisotropy energy. As indicated by Shapira [11], The AF→SF transition occurs at

$$B_{SF} = [2K/(\alpha - \chi)]^{1/2}, \quad (6)$$

where K is the effective anisotropy energy per unit mass, α is the susceptibility in the SF phase and χ is the susceptibility in the P phase. It equation can be rewrite as,

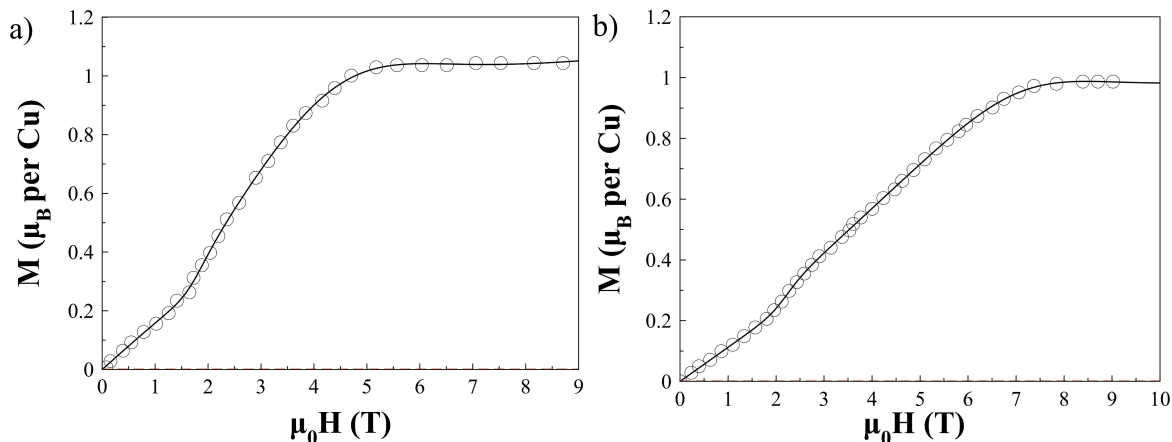


FIGURE 2. The solid line represents the best fits with Eq. (5). The open circles are 2 K data on polycrystalline a) $\text{Ba}_3\text{Cu}_3\text{In}_4\text{O}_{12}$ and b) $\text{Ba}_3\text{Cu}_3\text{Sc}_4\text{O}_{12}$ taken from Ref. 14.

TABLE II. Parameters obtained for $\text{Ba}_3\text{Cu}_3\text{In}_4\text{O}_{12}$ and $\text{Ba}_3\text{Cu}_3\text{Sc}_4\text{O}_{12}$ compounds with Eq. (5). Numbers in parentheses are statistical errors. The μ parameters for Cu^{2+} were taken from Ref. 14.

Compound	χ ($\times 10^{-7}$)	α ($\times 10^{-7}$)	M_0 (A/m) ($\times 10^{-7}$)	M_s ($\mu\text{B}/\text{Cu}$)	B_{SF} (T)	B_P (T)	σ_{SF} (T)	σ_P (T)	Ref.
$\text{Ba}_3\text{Cu}_3\text{In}_4\text{O}_{12}$	2.05(6)	3.5(2)	-2.0(6)	1.24(1) 1.05	1.7(1) 1.7	4.5(2) 3.9	0.4(1)	1.9(2)	* [15]
$\text{Ba}_3\text{Cu}_3\text{Sc}_4\text{O}_{12}$	1.41(2)	1.79(2)	-0.08(9)	1.12(2) 1.0	2.16(4) 2.1	7.2(2) 6	0.38(6)	1.9(1)	* [15]

*This work.

$$K = [(\alpha - \chi)(B_{SF})^2]/2. \quad (7)$$

Thus, the values for K at various temperatures were calculated from Eq. (7) (see Table I). For above of 10 K, the values for susceptibility α in the SF phase are higher than the susceptibility χ in the AF phase, as expected. However, for 2 and 4 K occurs the contrary. It means that at these temperatures the thermodynamic potential (from Eq. (6) in Ref. 11) in the AF phase is higher than the thermodynamic potential in the SF phase. It is usually found that magnetic materials that have a larger symmetry leads to lower anisotropy, so materials with cubic crystal structure have lower anisotropy energy than hexagonal materials. Thus, the effective anisotropy energy of $\text{BaFe}_{12}\text{O}_{19}$ with hexagonal structure is 4.7×10^6 erg/cm³ [12]. In our case, for $\text{Ag}_2\text{FeGeSe}_4$ with a pseudo-cubic structure and using the density value (6.83×10^3 kg/m³), we have obtained anisotropy energy values of order 10^3 erg/cm³, *i.e.*, of same order that Ni (cubic structure) [13].

Since for $\text{Ag}_2\text{FeGeSe}_4$ the saturation of the magnetization was not reached experimentally, in order to test the present model in the region of high fields where the magnetization saturates, M(B) curves for $\text{Ba}_3\text{Cu}_3\text{In}_4\text{O}_{12}$ and $\text{Ba}_3\text{Cu}_3\text{Sc}_4\text{O}_{12}$ compounds recently reported [14] were fitted using Eq. (5). The obtained parameters are summarized in Table II. It can be seen that the values for B_P and B_{SF} obtained for these compounds agree quite well with those reported. Also, their widths σ_{SF} and σ_P are reasonable physi-

cally. As expected, the thermal broadening for the transition SF→P is greater than that for the transition AF→SF. These results confirm the validity of the present model. Kumar *et al.* [15] used a microscopic 1D model of the P phase combined with a phenomenological model based on sublattice magnetization for crystals with SF or AF transitions that describes the magnetization curve and that only provides information on critical field strengths of the transitions.

In summary, we have shown that the scheme proposed by Ehrenberg *et al.* [7] to study the temperature and magnetic field dependence of magnetization in the AF, SF and P phases of the low anisotropy antiferromagnetic materials, success describe all magnetization curves below Néel temperature for the $\text{Ag}_2\text{FeGeSe}_4$ compound. In the present case, for the analysis of the paramagnetic region, the model was adapted for polycrystalline samples by using the classical Langevin function instead of the Brillouin one normally used for single crystals. Transitions given by B_{SF} and B_P , lead to the magnitudes χ , α , σ_{SF} , σ_P and K in Table I. The parameters χ , α , σ_{SF} , σ_P and K provide a consistent picture and a starting point for more detailed studies of the magnetic interactions in this type of compounds.

Acknowledgments

This work was partially supported by the Consejo de desarrollo Científico, Humanístico, Tecnológico y de las Artes de la Universidad de Los Andes (CDCHT-ULA Project No. C-1875-14-05-B).

1. W. Schäfer and R. Nitsche, *Mater. Res. Bull.* **9** (1974) 645-654.
2. M. Quintero, A. Barreto, and P. Grima, *Mater. Res. Bull.* **34** (1999) 2263-2270.
3. H. Katagiri *et al.*, *Thin Solid Films.* **517** (2009) 2455-2460.
4. Y. Shapira, E. McNiff, N. Oliveira, E. Honig, K. Dwight, and A. Wold, *Phys. Rev. B.* **37** (1988) 411-418.
5. G. McCabe *et al.*, *Phys. Rev. B.* **56** (1997) 6673-6680.
6. J.C. Woolley *et al.*, *J. Magn. Magn. Mater.* **257** (2003) 87-94.
7. H. Ehrenberg, H. Weitzel, H. Paulus, and H. Weitzel, *J. Magn. Magn. Mater.* **186** (1998) 74-80.
8. K.W. Blazey, H. Rohrer, and R. Webster, *Phys. Rev. B.* **4** (1971) 81-87.
9. Y. Shapira and S. Foner, *Phys. Rev. B.* **1** (1970) 3083-3096.
10. K.W. Blazey and H. Rohrer, *Phys. Rev.* **173** (1968) 574.
11. Y. Shapira, *J. Appl. Phys.* **42** (1971) 1588-1594.
12. X. Batlle *et al.*, *J. Appl. Phys.* **74** (1993) 3333-3340.

13. B.D. Cullity and C.D. Graham, *Introduction to Magnetic Materials*, 2nd Edition, (Wiley-IEEE Press, 2008).
14. S.E. Dutton, M. Kumar, Z.G. Soos, C.L. Broholm, and R.J. Cava, *J. Phys. Condens. Matter.* **24** (2012) 166001.
15. M. Kumar, S.E. Dutton, R.J. Cava, and Z.G. Soos, *J. Phys. Condens. Matter.* **25** (2013) 136004.